Supporting Information

Customized A-D-A type molecule to construct nitric oxide nanogenerator with enhanced antibacterial activity for infected wound healing

Yunxia Wang,[a] Xiaohuan Wang,[a] Chuangxin Zhang,[a] Ruipeng Li,[a] Jing Li,[a] Hu Shi,[a] Caihong Zhang,[a] and Liheng Feng*[a,b]*

[a]School of Chemistry and Chemical Engineering, Shanxi University, Taiyuan, 030006, P.R. China

[b]Institute for Carbon-Based Thin Film Electronics, Peking University, Shanxi (ICTFE-PKU), Taiyuan 030012, P.R. China.

E-mail: chzhang@sxu.edu.cn; lhfeng@sxu.edu.cn.

1. Experimental Sections

Materials and measurements. 2,7-dibromofluorene, 1,6-dibromohexane, Tetrabutylammonium bromide (TBAB), 5-bromo-2-(3,4-vinyldioxythiophene) formaldehyde, potassium acetate, 1,3-Bis(dicyanomethylene)indan, 1,3-Indanedione, 3-Dicycanovinylindan-1-one, bis(pinacolato)diboron, K_2CO_3, tetratriphenylphosphine palladium and $PdCl_2$(dppf) were obtained from Anhui Zesheng Technology Co., Ltd. BNN6 and Human Serum Albumin (HSA) were obtained from Shanghai yuanye Bio-Technology Co., Ltd. 2,7-Dichloro-Dihydrofluoresceindiacetate (DCFH-DA), Dihydroethidium (DHE), Hydrogen Peroxide Assay Kit, Aminophenyl fluorescein (APF), 1,3-Diphenylisobenzofuran (DPBF) were obtained from Shanghai Maokang Biotechnology Co., Ltd. LB nutrient agar, nutrient agar (NA) and trypticase soy broth (TSB) were obtained from Qingdao Hope Bio-Technology Co., Ltd. *S. aureus* (ATCC 6538) was obtained from China National Center for Microbial Culture Preservation and Management. NMR and MS spectra were obtained on Bruker AVANCE III HD series spectrometer and ultrafleXtreme MALDI-TOF/TOF (Germany). UV-Vis absorption spectra and fluorescence emission spectra were measured using Hitachi UH5300 and F-4600 spectrophotometers (Japan). Hydrated particle size distribution and zeta potentials were recorded by a Winner 802 analyzer (China) and Malvern Nano ZS90 (America). TEM images of the material were obtained using a JEOL JEM-F200. Fluorescence images of microbes were obtained on a Zeiss LSM 880 confocal laser scanning microscope (Germany).

Calculation of photothermal conversion efficiency. The photothermal conversion efficiency (η) of materials was according to the formula as follows:

$$\eta = \frac{hS(\triangle T_{max} - Q_{Dis})}{I\left(1 - 10^{-A_{660}}\right)} \qquad (1)$$

$$hS = \frac{m_D C_D}{\tau_s} \qquad (2)$$

$$\tau_s = -\frac{t}{ln\theta} \qquad (3)$$

$$\theta = \frac{T - T_{surr}}{T_{max} - T_{surr}} \qquad (4)$$

In the equation (1), h is the heat transfer coefficient; S *is* the heated surface area; $\triangle T_{max}$ represents the maximum temperature difference and is calculated from T_{max}-T_{surr} (T_{max} and T_{surr} represent the maximum temperature and ambient temperature, respectively); I represents laser power and A_{660} is the absorbance intensity of sample at 660 nm. In the equation (2), m_D and C_D represent the mass and heat capacity of water, respectively.

2. Supporting Figures

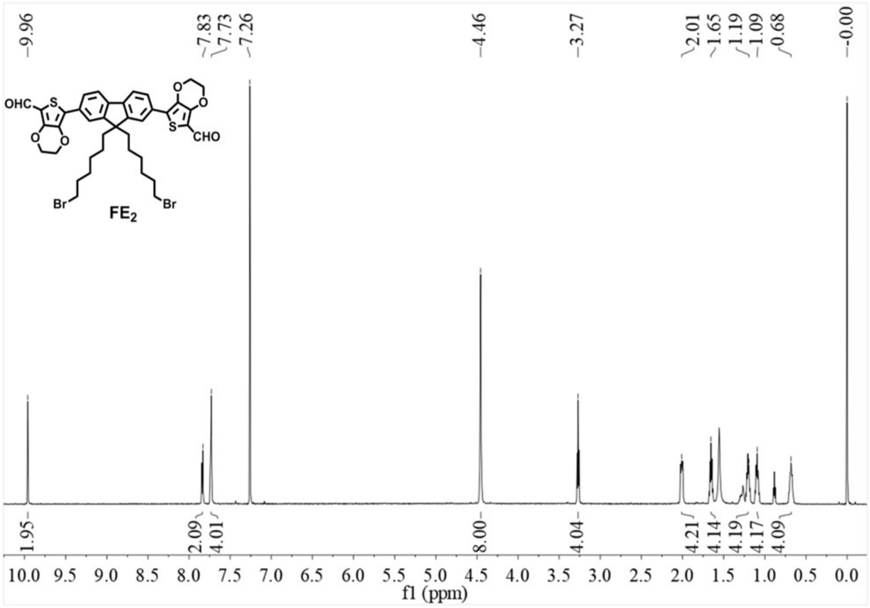

Figure S1. ^{1}H NMR spectrum of FE_2 in $CDCl_3$.

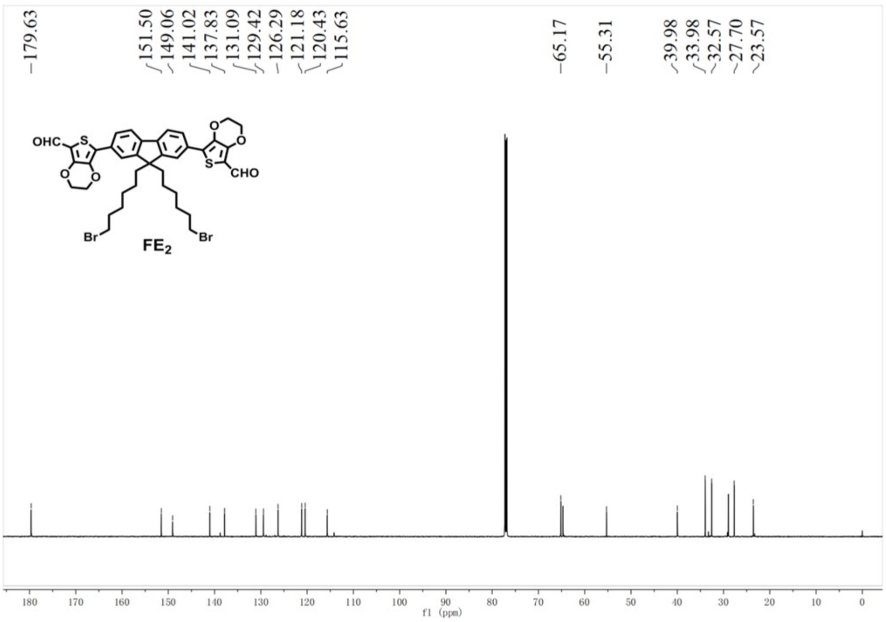

Figure S2. ^{13}C NMR spectrum of FE_2 in $CDCl_3$.

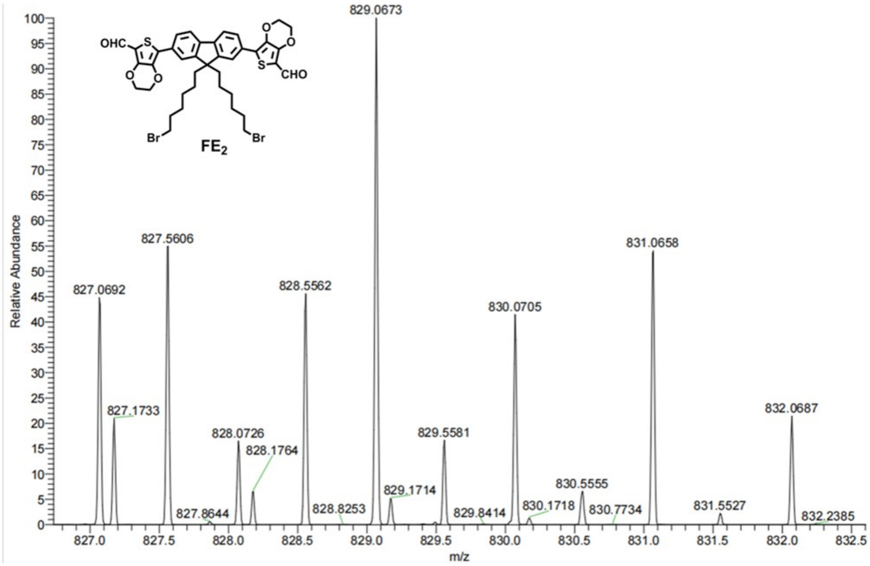

Figure S3. HRMS-ESI spectrum of FE_2.

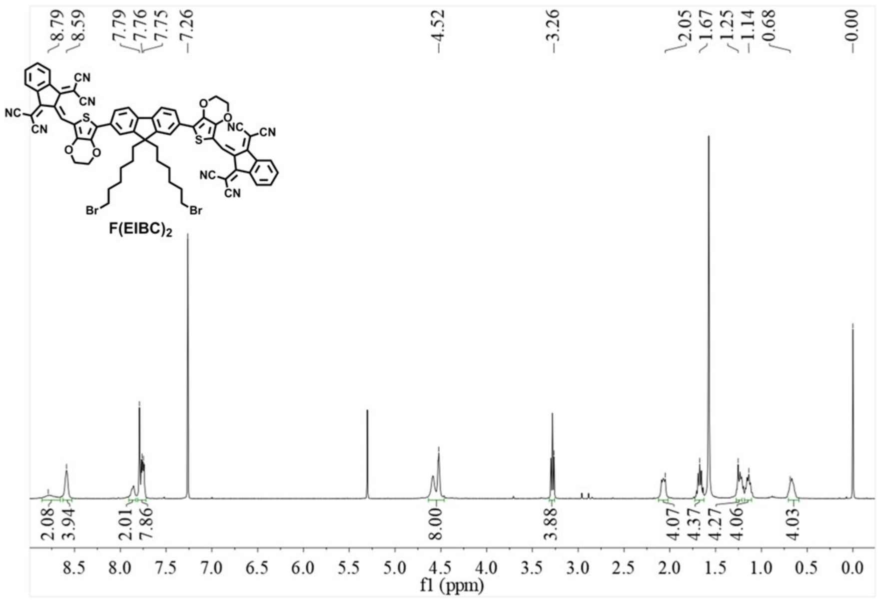

Figure S4. ^{1}H NMR spectrum of $F(EIBC)_2$ in $CDCl_3$.

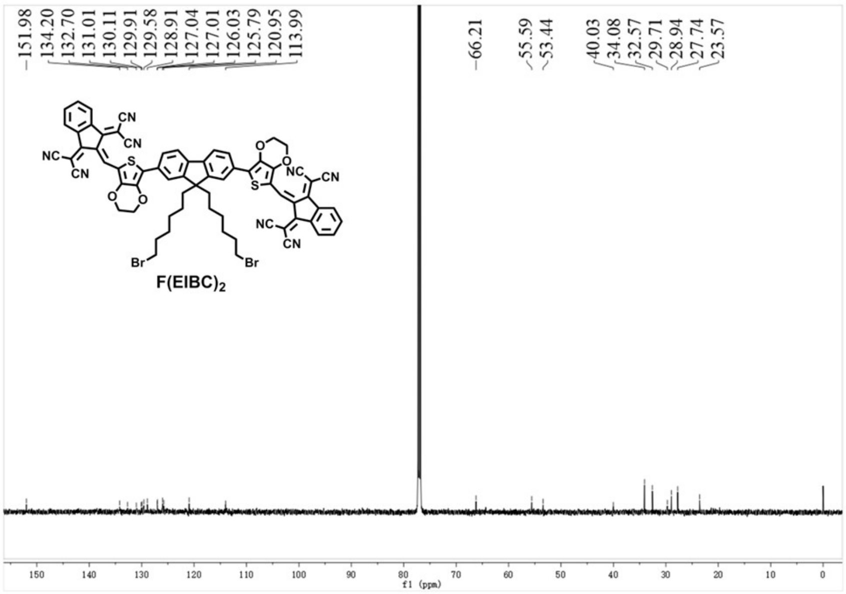

Figure S5. ^{13}C NMR spectrum of $F(EIBC)_2$ in $CDCl_3$.

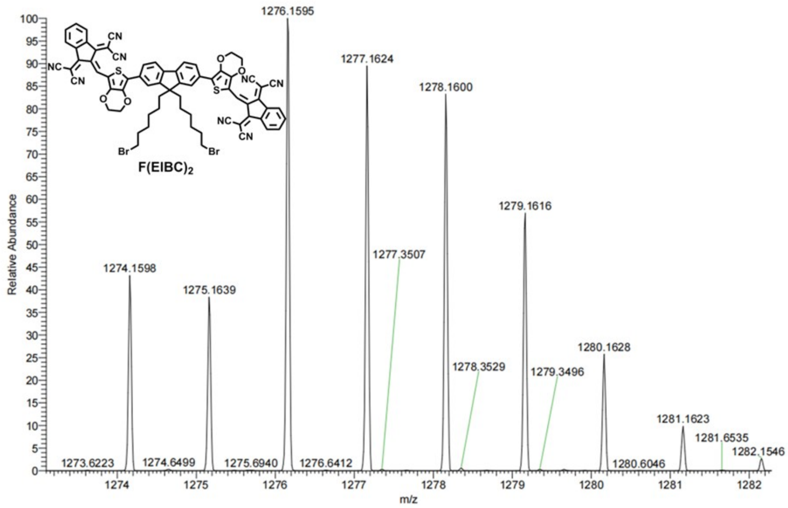

Figure S6. HRMS-ESI spectrum of $F(EIBC)_2$.

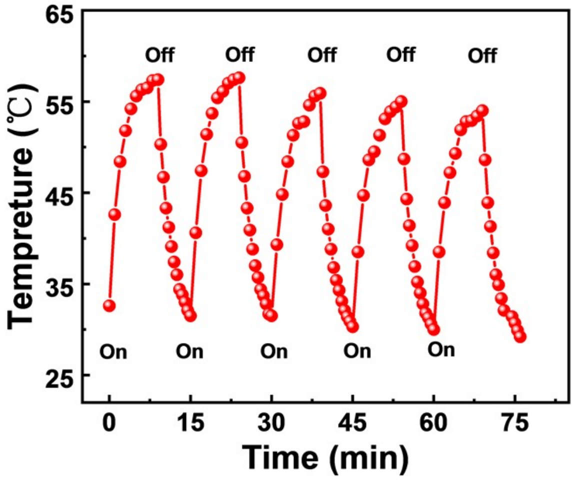

Fig. S7. The photothermal stability measurement of $F(EIBC)_2$ using a 660 nm laser (1 W/cm^2).

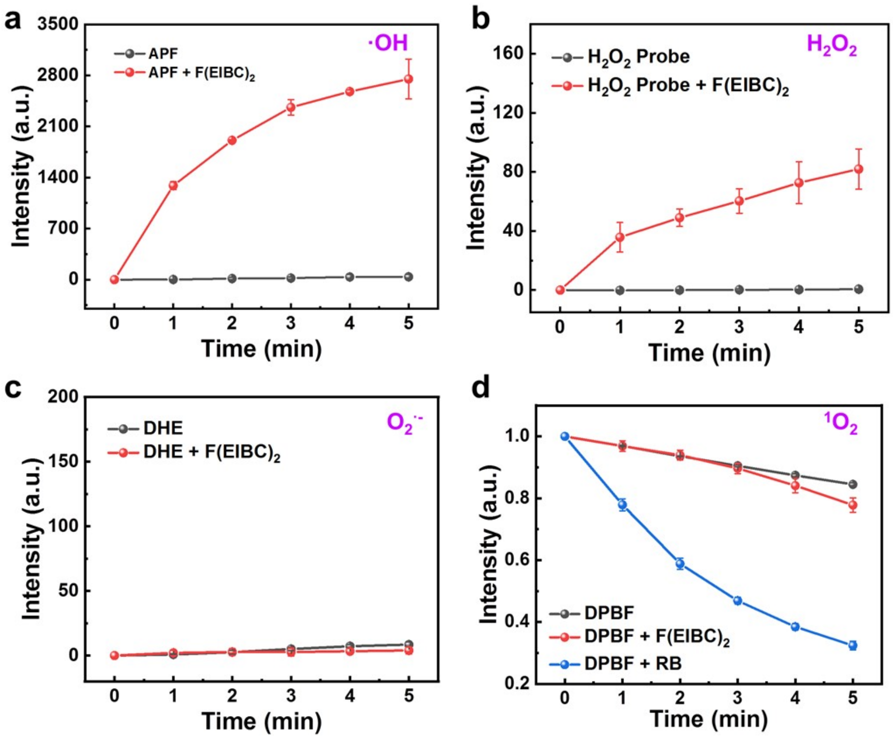

Fig. S8 The measurement of generation of a) ·OH, b) H_2O_2, c) $\cdot O_2^-$ and d) $^1O_2$ from irradiated $F(EIBC)_2$ using a 660 nm laser (1 W/cm^2).

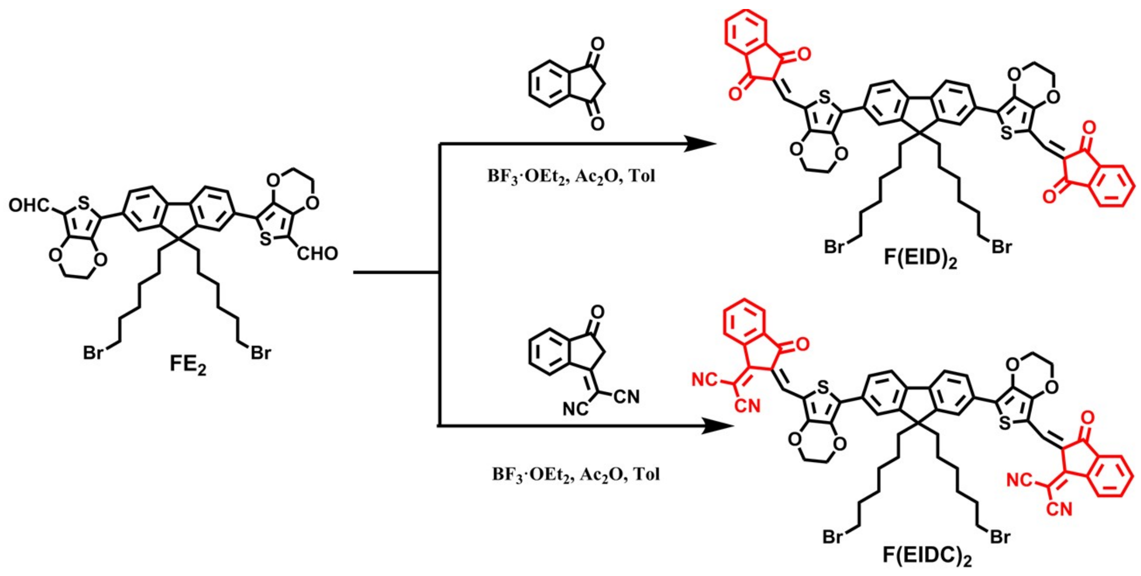

Fig. S9 Synthetic route of F(EID)$_2$ and F(EIDC)$_2$.

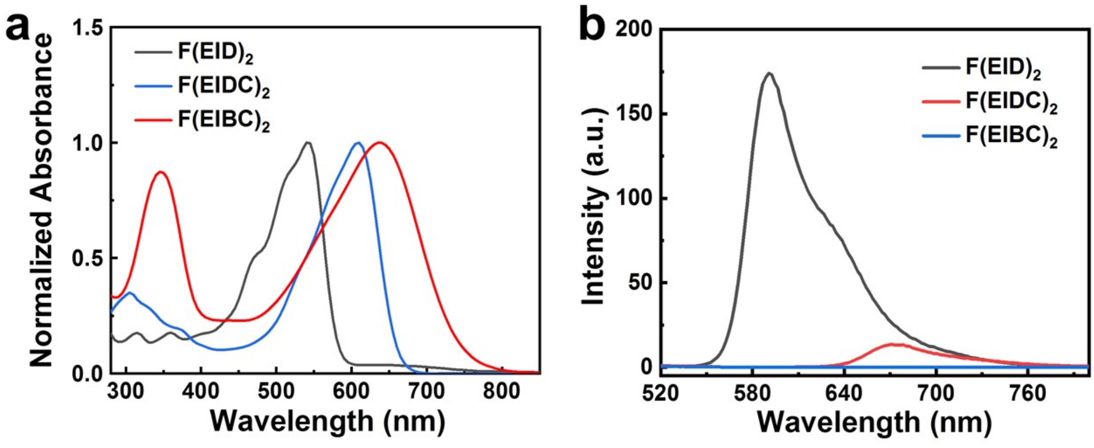

Fig. S10 a) Normalized absorption spectra of three molecules. b) Fluorescent spectra of three molecules.

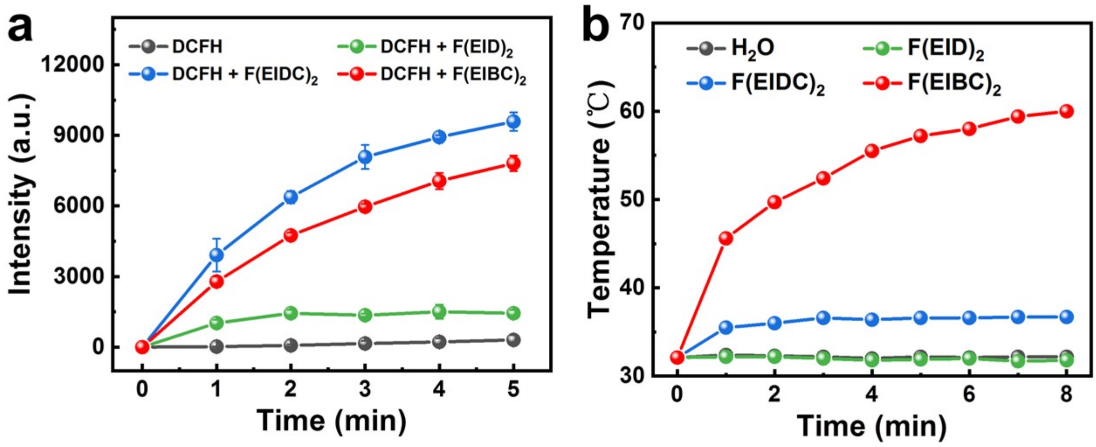

Fig. S11 a) ROS generation detection of three molecules. b) Photothermal property test of three molecules.

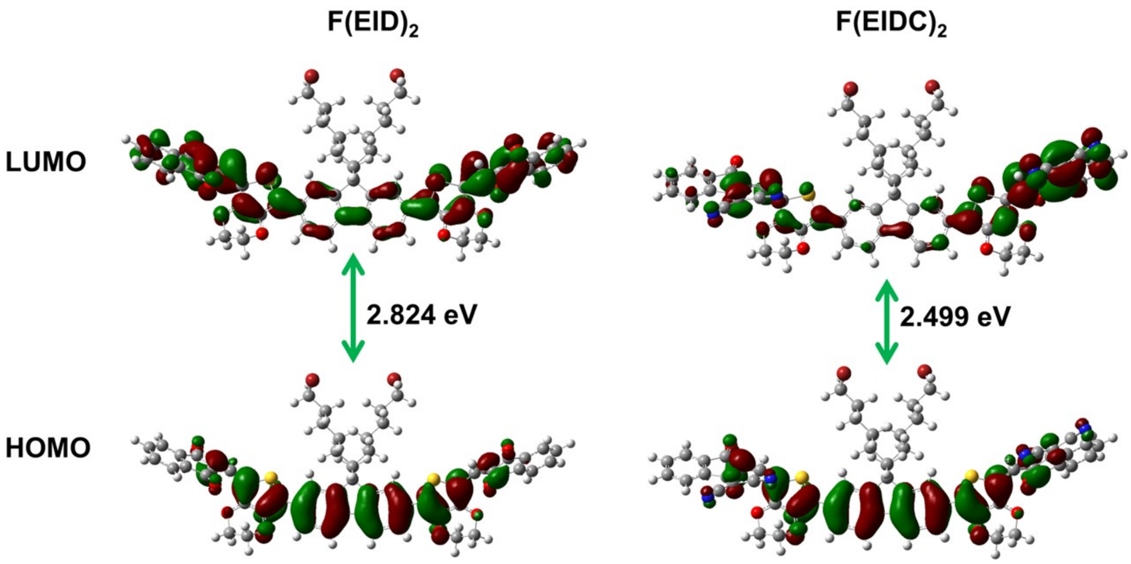

Fig. S12 The HOMO-LUMO distributions and optimized geometries of $F(EID)_2$ and $F(EIDC)_2$.

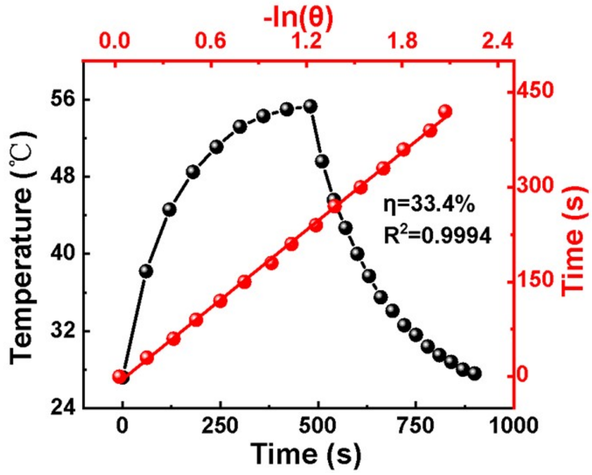

Fig. S13 Photothermal response of HFB solution (10 μM) under light irradiation of a 660 nm laser (1 W/cm^2) for 8 min followed by removing the laser.

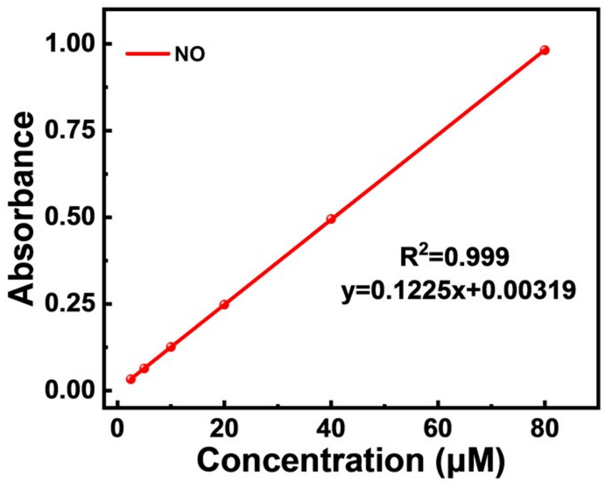

Fig. S14 The NO standard curve established by $NaNO_2$ aqueous solution.

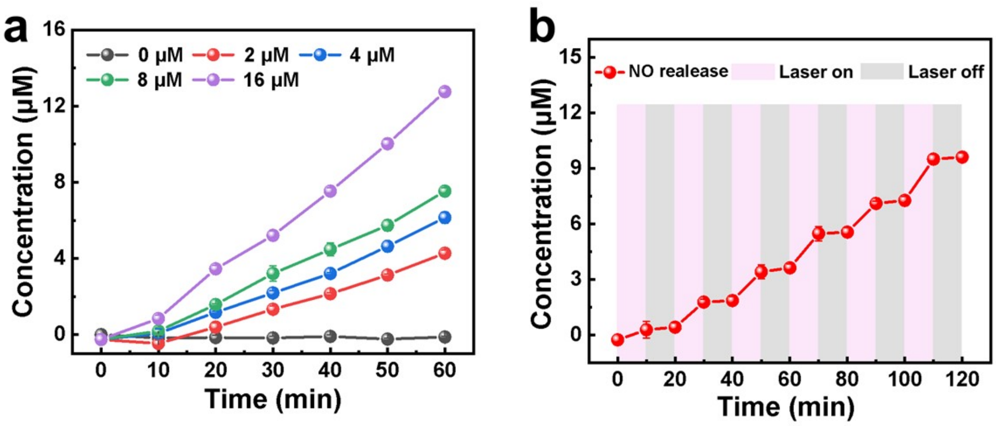

Fig. S15 The measurement of NO generation a) at different concentrations of HFB under light irradiation and b) during 6 light on-off cycles. Light: 660 nm laser; 1 W/cm^2.

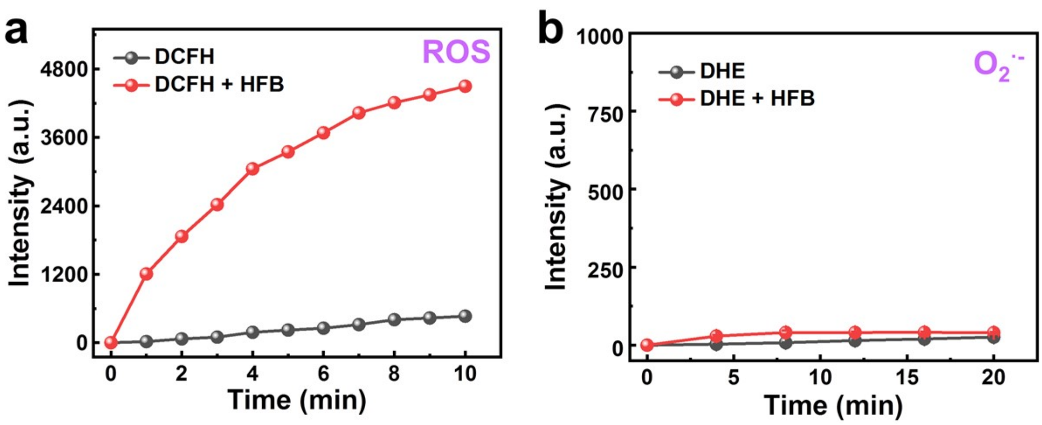

Fig. S16 The measurement of a) total ROS and b) $\cdot O_2^-$ generated by HFB under a 660 nm laser irradiation (1 W/cm^2).

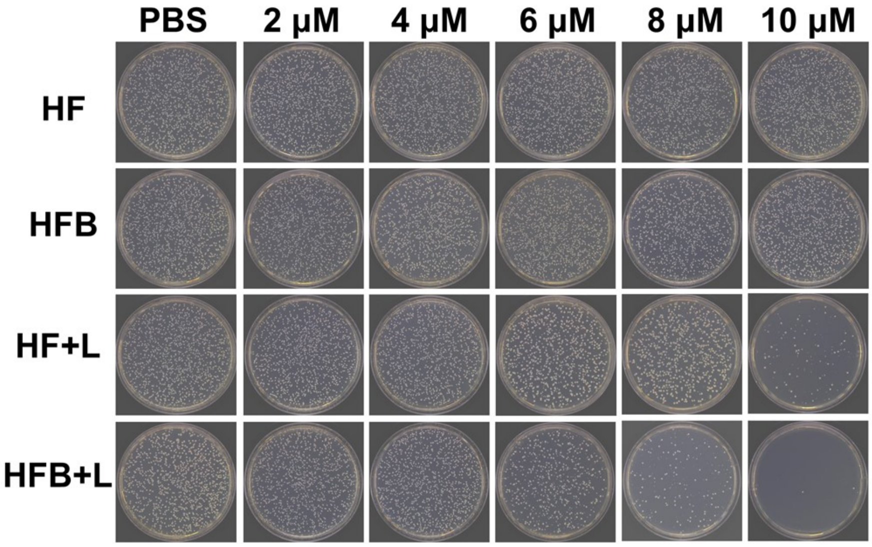

Fig. S17 The representative photographs of *S. aureus* colonies grew on agar plates after different treatments.

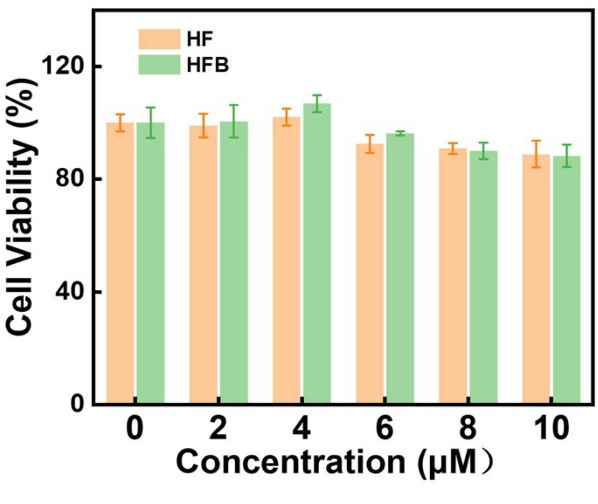

Fig. S18 Cell viability of L929 cells after different treatments.

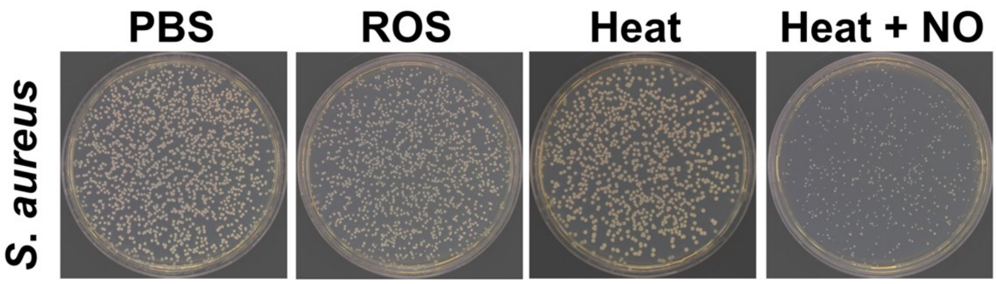

Fig. S19 The representative photographs of *S. aureus* colonies grew on agar plates after different type of damages.

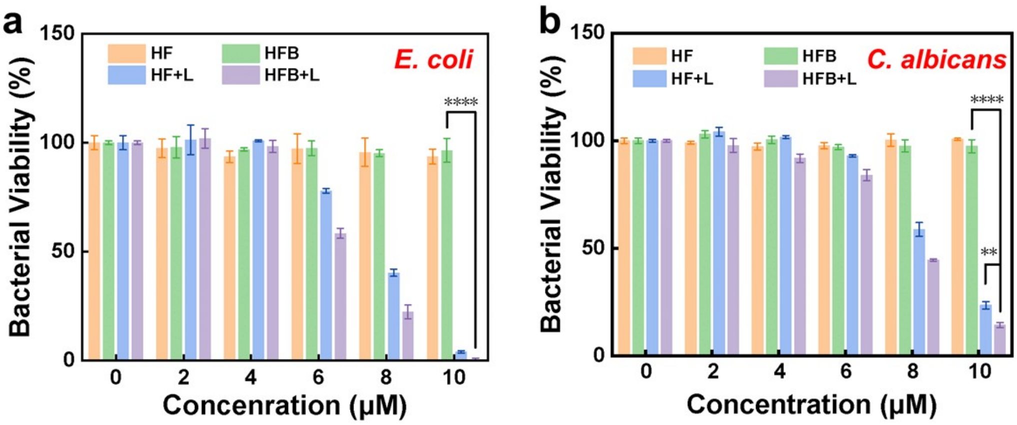

Fig. S20 In vitro antimicrobial activity of HFB toward a) *E. coli* and b) *C. albicans*.

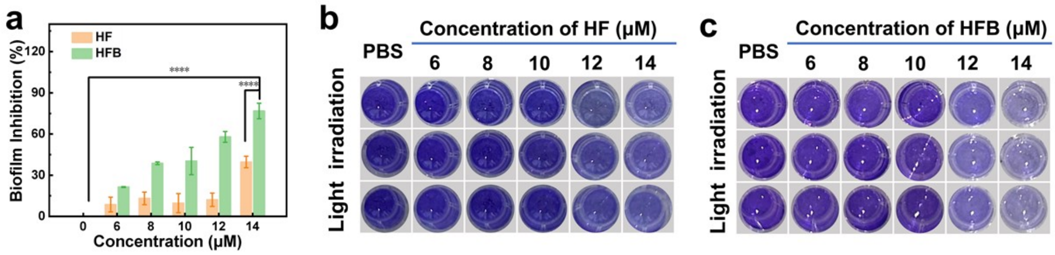

Fig. S21 a) The measurement of *S. aureus* biofilm inhibition of different concentrations of HF and HFB under laser irradiation (1 W/cm^2). The representative photos of biofilms stained by crystal violet after treatment of irradiated b) HF and c) HFB.

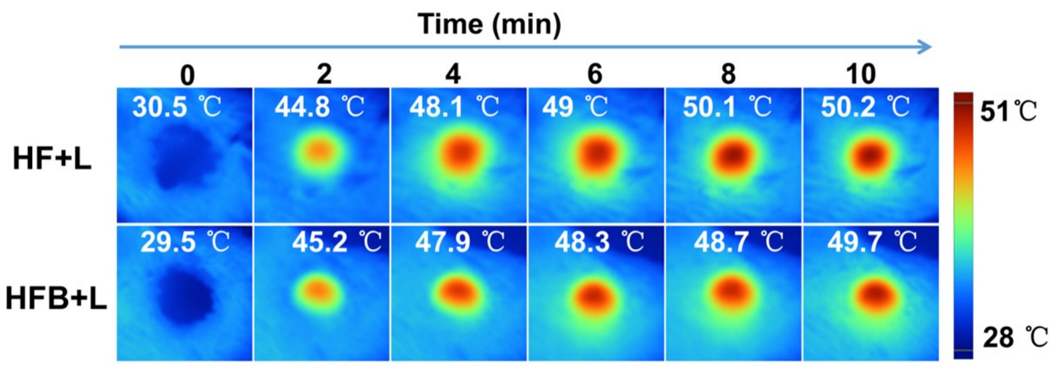

Fig. S22 The photothermal images of infected wound of mice under different treatments at different time points.

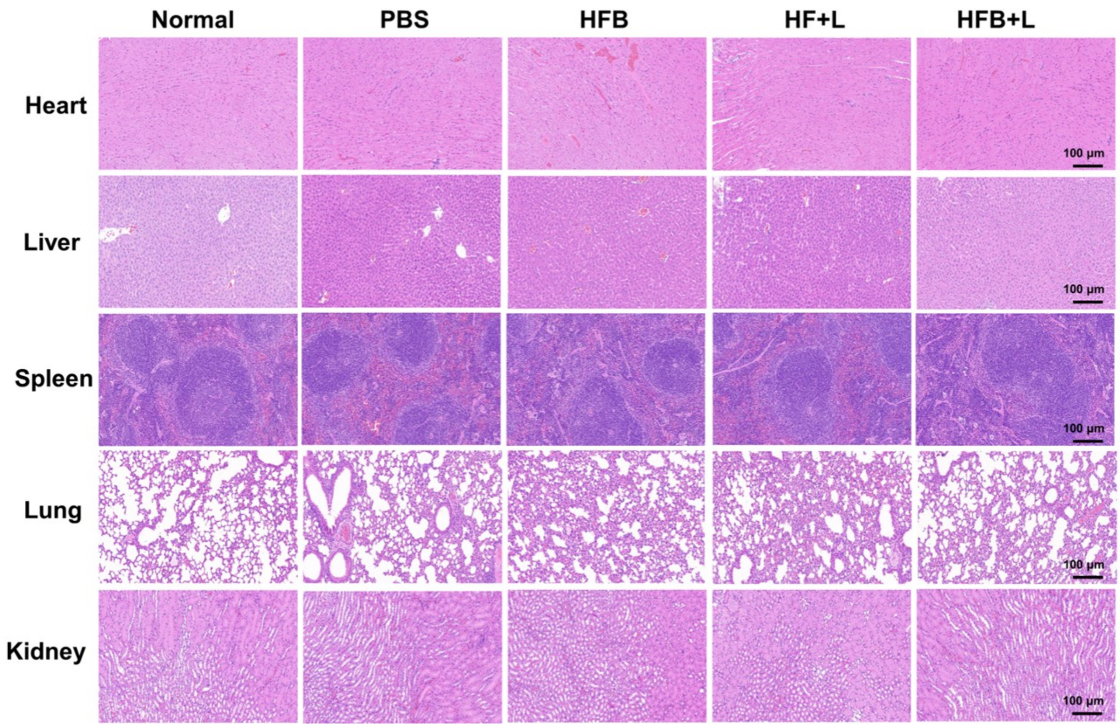

Fig. S23 The H&E staining of major organs of mice after different treatments.